

Effect of Partial Diffusion on Current–Time Transients and Throughputs for Reactions at Rough Surfaces

Rengaswamy Srinivasan* and Hassan M. Saffarian

Applied Physics Laboratory, The Johns Hopkins University, Laurel, Maryland 20723-6099

Received: October 8, 2001

Conventional theories of electrochemical kinetics, which are strictly applicable for two-dimensional surfaces, predict that the current (I) increases indefinitely with an increase in the reaction rate constant (k_f), limited only by diffusion. By comparison, the I – t transients behave differently on electrodes with a rough and porous surface (dimension, $D_f > 2$) than on electrodes with a flat surface ($D_f = 2$). The difference in the behavior is caused by the flux of the reactant toward the porous surface. The rate expression for the porous electrode is obtained under the mass transfer conditions of partial diffusion in terms of D_f and k_f , by extending the well-known I – t behavior for the planar electrode. The expression predicts that for a porous electrode, the currents in I – t transients have higher values at higher k_f , but only when t is close to zero. At longer times, however, the currents are higher at lower k_f , where the rate is limited by partial diffusion, than at higher k_f , where the rate is limited by total diffusion. The implications of long-term behavior of current and the associated charge (Q) are discussed in the context of electrochemical reactors such as fuel cells.

Introduction

Surface reactions in fuel cells and other catalytic reactors commonly occur at the interfaces between two or more phases. The physicochemical properties of catalyst surfaces are carefully designed such that the activation energy is most favorable for the desired reaction, as in the case of Pt electrodes used for reducing oxygen and oxidizing hydrogen in fuel cells. Most catalysts are designed with a rough surface and porous body, with a dimension (D_f) that is greater than 2. This allows a catalyst to have a true surface area (A) much greater than its geometric surface area (G), which allows the catalyst to maximize the rate of consumption of the reactants.¹ However, in most fuel-cell-type reactors the rate enhancement is far less than what one would expect from the ratio of A/G , which is commonly known as roughness factor. In other words, only a fraction of A , which we call the effective area, A' , influences the reaction. Although there are a number of factors that can contribute to less-than-optimum performance of a catalyst, a part of it is due to the influence of diffusion on A' . Diffusion plays a significant role in the kinetics of those reactions in which the activation energy is kept small by the electronic properties of the catalyst, or when the free energy is made largely negative by the application of an electrochemical potential (E); in an electrochemical system, E (related to the overpotential, η) influences the forward rate constant, k_f .²

For small k_f (large activation energy), the activation process will limit the rate of the reaction, and the surface concentration of the reactant will be close to the bulk concentration. Under these conditions, the rate of mass transfer of the reactant from the electrolyte to the surface of the electrode does not affect the overall rate of the reaction. Nevertheless, catalysts in reactors are generally designed to operate at large k_f values in order to maximize the rate of consumption of the reactant. If k_f is large, then mass transfer by diffusion will set in, and at extremely large values of k_f the rate of the reaction will be limited by the kinetics of diffusion.

In a reactor, as diffusion begins to dominate the reaction rate, the A' decreases, eventually reaching the limit G ; note that before the reaction starts ($t = 0$) $A' = A$. The rate at which A' changes with t depends on the rate at which the diffusion layer moves away from the electrode surface, except for a two-dimensional electrode (defined as $D_f = 2$), where $A = G$ for all t , and A' is independent of t . It is also common knowledge that k_f influences the rate of consumption of the reactant, which can be measured in terms of charge, Q . We will demonstrate in the following sections the interdependence of D_f , k_f , and diffusion, and how they influence Q . We will also show that the reaction on a rough surface can occur with maximum efficiency (or Q), not when k_f is so large that the rate is limited by diffusion, but when k_f is actually much smaller.

First, we demonstrate the pronounced effect of diffusion on A' through the electrochemical redox reaction, $\text{Fe(CN)}_6^{4-} = \text{Fe(CN)}_6^{3-} + \text{e}^-$. As a “fast” electrochemical reaction with a large standard rate constant (k_0), its rate is limited by diffusion at virtually all potentials (E).³ When this reaction is conducted on Pt surfaces with different roughness factors, the currents are indeed different as expected, but only at the start of the reaction when the potential is first applied (Figure 1). At longer times ($t > 0.25$ s), the currents merge with each other and the charges associated with the reaction are virtually identical between the smooth and rough electrodes, although the surface areas at the two extremes of roughness vary by a factor of 33.

An explanation of this behavior is that at the start of the reaction, the nascent diffusion layer has essentially the same area as the underlying electrode surface and the initial current reflects the differences in dimensionality. Thus, for the rough electrode, at initial times, the current is indeed higher than the current for the smooth electrode. As the reaction proceeds, the diffusion layer moves away from the surface and the dimensionality of the diffusion layer approaches a planar geometry at longer times. Eventually, the current becomes equivalent for all the electrode types, independent of their initial roughness.

A schematic of the time-dependent increase of the diffusion layer thickness (δ) is depicted in Figure 2. It is generally

* Corresponding author.

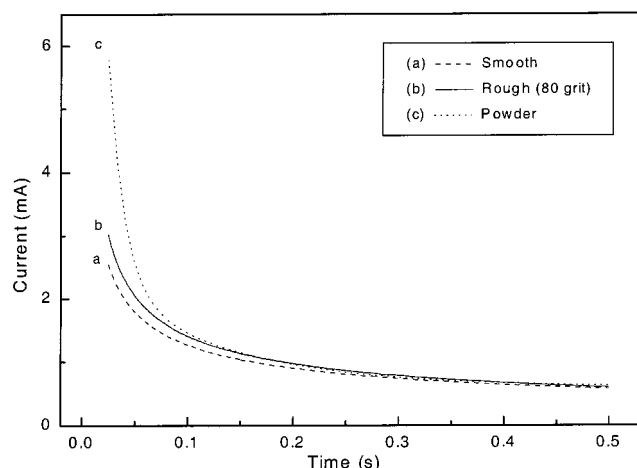


Figure 1. I - t transients at 0.7 V (vs RHE) for oxidation of 15 mM $\text{Fe}(\text{CN})_6^{4-}$ in aqueous 3 M NaNO_3 on Pt electrodes with $G = 0.283 \text{ cm}^2$: (a) smooth surface ($D_f = 2.0$); mean height (h) within $100 \times 100 \text{ nm}$ sampled areas = 10 nm; (b) roughened surface ($D_f = 2.08$; $h = 100 \text{ nm}$); and (c) fuel-cell catalyst-type, prepared from Pt powder ($D_f = 2.44$; $A = 33 \times G$; $h = 2 \mu\text{m}$). The charge Q between 300 and 1000 ms was 369, 381, and $387 \mu\text{C}$ for the smooth, rough, and catalyst (roughest) electrodes, respectively.

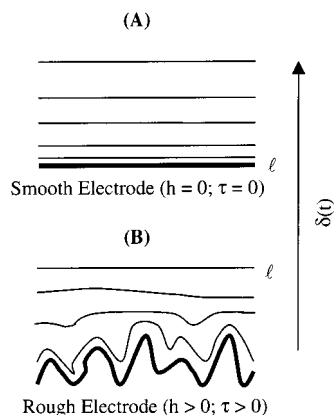


Figure 2. Schematic of the time-evolution of the diffusion layer thickness, δ , which varies as $(\pi Dt)^{1/2}$. l is the limit of δ when the diffusion layer boundary reaches a planar (2-D) geometry. For a fast reaction ($k_0 > 2 \times 10^{-2} \text{ cm/s}$), the rate is instantly limited by diffusion. On a smooth electrode ($D_f = 2.0$), $\delta \rightarrow l$ for all values of $t > 0$. On a rough electrode, ($2 < D_f < 3$), $\delta \rightarrow l$ when $t \gg \tau$, where τ is defined as the time for δ to reach the mean height, h .

assumed that $\delta = (\pi Dt)^{1/2}$ under the conditions of semi-infinite linear diffusion on a planar surface.⁴ If we define τ as the time taken for δ to reach the limit of the height (h) associated with surface roughness, then it will occur virtually instantaneously on a planar surface. In this case, the cross section of the diffusion layer will have a planar geometry at all times, beginning at $t = 0$. For the rough catalyst-type Pt with $h = 2 \mu\text{m}$ (h estimated by scanning tunneling microscopy) at $t = 0$, the diffusion layer would resemble the topography of the electrode surface. When diffusion begins, the boundary of the diffusion layer would move farther and farther away from the surface, and it will resemble less and less of the surface topography. When the current, I , for the rough electrode merges with that of the planar electrode, at that time the diffusion layer associated with the rough electrode may be considered as having reached a planar geometry. On the basis of this assumption, for the $\text{Fe}(\text{CN})_6^{4-}$ oxidation reaction (Figure 1), it takes about 0.25 s for the diffusion layer associated the roughest electrode to attain a planar geometry. Assuming $D = 5 \times 10^{-6} \text{ cm}^2/\text{s}$ for $\text{Fe}(\text{CN})_6^{4-}$,

in 0.25 s, δ would reach about $20 \mu\text{m}$. Thus, when δ reaches a distance of about $10 \times h$, the reactant approaching from the bulk appears to “see” no more than the geometric area, G , of the electrode. We define this limit of δ as l , when the diffusion plane has a planar geometry, with a cross-sectional area essentially equivalent to G . Beyond this limit charges associated with the reaction are similar on both the smooth and rough surfaces. The model described above provides a qualitative explanation for the nondependence of Q on A , when k_0 is so large that the reaction rate is limited by diffusion.

The kinetics of the typical fuel cell reaction involving oxygen reduction on Pt is, however, much different from that of $\text{Fe}(\text{CN})_6^{4-}$ oxidation on Pt. The oxygen reduction reaction has a smaller rate constant ($k_0 \ll 1 \times 10^{-2} \text{ cm/s}$), and its rate is only partially limited by diffusion over a wide range of potentials.⁵ In this case, the rate of change of δ with t is expected to be much smaller than for the fast reaction, and it will depend on not only the diffusion coefficient of the reactant, D , but also on k_f . Furthermore, the time taken for δ to reach the limit l can be substantially longer than (the faster) $\text{Fe}(\text{CN})_6^{4-}$ oxidation. Most important, as the rate of change of δ with t gets smaller, the time-dependent change of the effective area available for the reaction will also be smaller, with desirable effects on I and Q . Note that in a fuel cell, larger I means greater power density and larger Q means greater energy density, which are two crucial parameters that define the performance of any power source. Therefore, constructing a fuel cell with due consideration for the interaction between D_f , k_f , and diffusion will help maximize both I and Q .

Electrochemists classically model reaction kinetics on rough electrodes, where rate is limited by either total activation/no diffusion⁶ or total diffusion.^{7–18} In this work, we propose a model for reactions on porous electrodes with dimension, $2 < D_f < 3$, in which rate can be limited by total activation, total diffusion, or partial diffusion. Such a model applies to reactions in fuel cells and other reactors that use rough and porous electrodes. We provide experimental verification under a broad range of rate conditions, using flat ($D_f = 2.0$) and porous ($D_f > 2.0$) electrodes.

Partial-Diffusion, Reaction Rate, and Porous Electrodes.

Several works attempt to understand the I - t and ac impedance behaviors of rough electrodes for reactions whose rates are under total diffusion limit.^{7–10} Pajkossy et al. studied the kinetics of diffusion-limited reactions on fractal electrodes with modeling and simulation,¹¹ and experiments on carefully designed fractal electrodes.¹² Sapoval et al. developed models to describe ac impedance behavior under steady-state diffusion for reactions on rough and porous surfaces. Sapoval’s numerical models are based on a Laplacian field obeying primary current distribution (Dirichlet boundary conditions) with coarse-grain modeling of the electrode geometry through finite element analysis. Work by Sapoval et al. addressed two computational issues: calculating shape (geometry) and transport parameters from a priori knowledge of the net flux to an electrode,¹⁰ and calculating flux using the shape of the electrode.¹³ Other studies model the behavior of a “quasi-reversible” reaction with the rate limited by “mixed” activation and diffusion on a planar surface modified through perturbations to represent a sinusoidal- or Gaussian-type “rough” surface.¹⁴ The short-time chronoamperometric behavior of diffusion-limited reactions on electrodes of “arbitrary” shapes has also been similarly addressed.¹⁵ Review articles by de Levie¹⁶ and Pajkossy^{17,18} summarize earlier studies on the electrochemical reactions on rough and porous electrodes. Unlike previous studies,^{7–18} the work presented below addresses not only reac-

tions with diffusion-limited rates, but also reactions with rates limited by partial-diffusion/partial-activation and full activation.

Most electrochemical reactions, including oxygen reduction on Pt, are not reversible and their rates, depending upon E , can be under either partial or total diffusion limit. In these cases, an analysis of the $I-t$ transient that accounts for the $A'-t$ relationship under slow diffusion provides a clue to the effect of surface roughness on I and Q .¹⁹

For a planar electrode under potentiostatic conditions, the general expression for $I-t$ transient for an irreversible reaction is^{20,21}

$$I(t) = (nFGC_b(D/t)^{1/2}) \lambda \exp(\lambda^2) \operatorname{erfc}(\lambda) \quad (1)$$

where $\lambda = k_f(t/D)^{1/2}$; n = number of equivalence; F = Faraday; and C_b = concentration of the reactant (oxidant) in the bulk of the electrolyte. As $\lambda \rightarrow \infty$ (i.e., either $t \rightarrow \infty$ or $k_f \rightarrow \infty$), $\lambda \exp(\lambda^2) \operatorname{erfc}(\lambda) \rightarrow 1/\pi^{1/2}$, and $I(t)$ takes the Cottrell form: $I(t) = nFGC_b(1/\pi)^{1/2}(D/t)^{1/2}$ for a reaction under the diffusion limit.^{22,23} As noted earlier, the term $(D/t)^{1/2}$ describes the rate of increase of δ with time. The Cottrell equation implies that $I(t)$ is independent of k_f and will continuously decrease with t due to the uninterrupted increase of δ . Furthermore, when the Cottrell equation is compared with eq 1, it is apparent that under the condition of total mass transfer limit, the rate of change of δ with t , and therefore the rate of change of I with t , will be at its maximum. On the other hand, for a slow reaction ($k_f \ll 1 \times 10^{-2}$ cm/s), where the reaction rate is under partial diffusion limit, the rate of change of δ with t will be much smaller.

To be able to use eq 1 for a reaction on a rough electrode, one has to replace the geometric area, G , in that equation with the true area, A . For example, A on Pt is obtained by the oxidation of adsorbed hydrogen, and on Au by the reduction of adsorbed oxygen.²⁴ Furthermore, we need to account for the influence of the electrode dimension, D_f , on the flux of the reactant, or the effective contribution by the $\exp(\lambda^2) \operatorname{erfc}(\lambda)$ term to I . We use a simple expression described by de Levie⁸ (see ref 8 for a survey of variation of de Levie's model) to relate D_f to the effective flux toward a rough surface. By combining the effect of D_f on flux and replacing G with A we extend eq 1 to

$$I(t) = nFC_b A k_f \exp(\lambda^{2\xi}) \operatorname{erfc}(\lambda^\xi) \quad (2)$$

where $\xi = (D_f - 1)$, and following de Levie,⁸ D_f is defined as the Hausdorff dimension. Equation 2 is a generalized $I-t$ expression for all conditions of $D_f \geq 2.0$. It is applicable to reaction rates under complete activation ($k_f \ll 1 \times 10^{-2}$ cm/s), diffusion ($k_f > 1 \times 10^{-2}$ cm/s), as well as mixed control. Equation 2 is rearranged as

$$I(t) = nFC_b(1/\pi)^{1/2} A (k_f^{(2-D_f)} (D/t)^{(D_f-1)/2}) (\pi)^{1/2} \lambda^\xi \exp(\lambda^{2\xi}) \operatorname{erfc}(\lambda^\xi) \quad (3)$$

Equation 3 leads us to several interesting conclusions. The term $(\pi)^{1/2} \lambda^\xi \exp(\lambda^{2\xi}) \operatorname{erfc}(\lambda^\xi)$, which describes the flux of the reactant to the rough surface, behaves analogously to $(\pi)^{1/2} \lambda \exp(\lambda^2) \operatorname{erfc}(\lambda)$ for the flat surface.²⁵ It follows a sigmoidal variation with λ^ξ , and changes from 0 to 1 as λ^ξ varies from small to large values (see Figure 3). Thus, under the conditions of diffusion limit, eq 3 reduces to

$$I(t) = nFC_b(1/\pi)^{1/2} A (k_f^{(2-D_f)} (D/t)^{(D_f-1)/2}) \quad (4)$$

Equation 4 is the Cottrell analogue for the rough electrode. When $D_f = 2$, eq 4 reduces to $I(t) = nFGC_b(1/\pi)^{1/2}(D/t)^{1/2}$, which is the Cottrell expression for the current under the

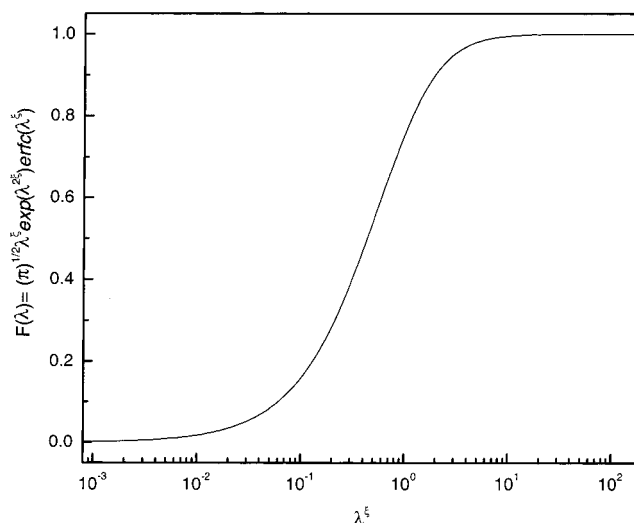


Figure 3. $(\pi)^{1/2} \lambda^\xi \exp(\lambda^{2\xi}) \operatorname{erfc}(\lambda^\xi)$ vs λ^ξ plot showing identical behavior for all values of D_f .

diffusion limit for flat electrodes. The term $(k_f^{(2-D_f)} (D/t)^{(D_f-1)/2})$ in eqs 3 and 4 indicates the increase of the diffusion layer thickness with time for all values of D_f . The time-dependent change of I in eq 4 can be described as

$$\log I(t) = \text{constant} - ((1 - D_f)/2) \log(t) \quad (5)$$

Note that the slope in eq 5 is $(1 - D_f)/2$ and is -0.5 only for a flat electrode ($D_f = 2$). For $D_f > 2$ (porous electrodes), the amplitude of the slope is between 0.5 and 1. Equation 5 is similar to the expression described by Pajkossy²⁶ for a diffusion-limited reaction on porous electrodes. Equation 4 assumes that the laws of semi-infinite linear diffusion are equally applicable for flat and rough electrode surfaces, as did the rate expression derived by Pajkossy and others.⁷⁻¹⁸

Furthermore, per eq 3, since $\lambda^\xi \exp(\lambda^{2\xi}) \operatorname{erfc}(\lambda^\xi)$ increases from 0 to 1 within the limit of $0 < \lambda^\xi < \infty$, I in the transients would always be higher at higher λ^ξ . However, its combination with the term $(k_f^{(2-D_f)} (D/t)^{(D_f-1)/2})$ has an interesting effect on $I-t$ transients: I is larger at all t at higher k_f , but only when $D_f = 2.0$. For $D_f > 2$, I is not necessarily higher at higher k_f , except when t is close to zero. The implications of the dependence of I on k_f and D_f in the context of fuel cell-type reactions are described next.

Limitation of Increasing k_f for Oxygen Reduction in Fuel Cells. First, we provide a graphical perspective of eq 3 through simulation of $I-t$ and $Q-k_f$ behaviors for a reaction that resembles oxygen reduction on surfaces with different roughness. As k_f changes from low to high values on a smooth electrode, the current in $I-t$ transients increases monotonically until I reaches the diffusion limit (Figure 4A). That is not the case for a rough electrode (Figure 4B), where it can be seen that the current that begins to increase with an increase in k_f decreases to lower values long before k_f becomes large enough to cause the rate to be limited by diffusion.

In the context of a fuel cell (and other electrochemical reactors), Q in Figure 4C represents the reactant consumed within a given time period, and therefore, the contribution of the reactant (such as oxygen) to the energy density of the fuel cell. Rough electrodes in those reactors are often constructed with the objective of maximizing the consumption of the reactant and increasing the throughput of the reaction over a given period of time. However, the ability to realize such an objective depends on the match between k_f and D_f . Note that the k_f at

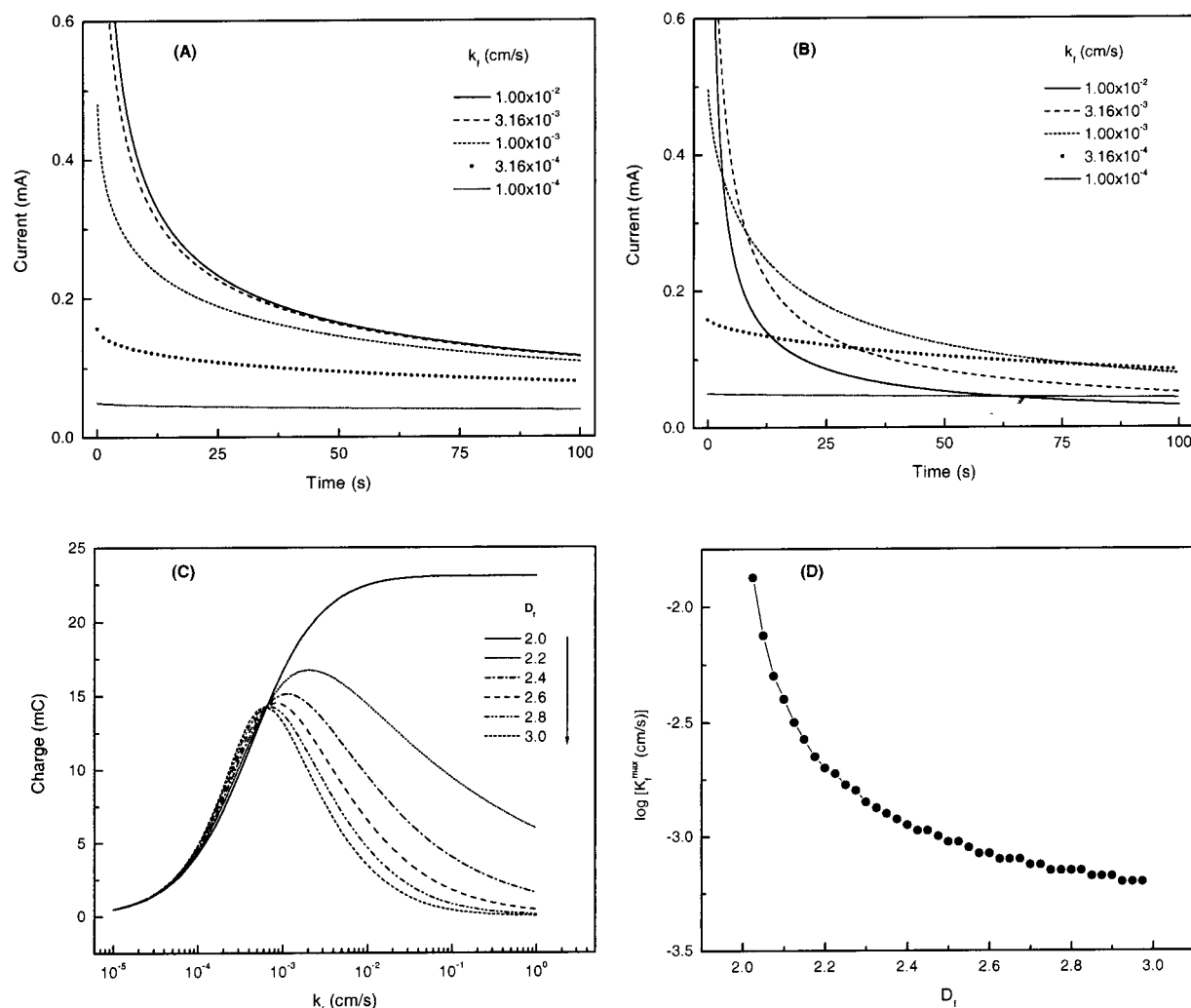


Figure 4. $I-t$ simulations using eq 3 for: (A) smooth ($D_f = 2$); and (B) rough ($D_f = 2.4$) surfaces for various values of k_f , as indicated; (C) $Q = \int_0^t I dt$ of the transient data ($t = 100$ s) in Figures 4A and 4B, and for several other D_f values; and (D) $\log(k_f^{\max})$ vs D_f . The true area (A) was assumed as identical ($A = 1$ cm²) for each D_f . Other parameters used in the simulation correspond to oxygen reduction on polycrystalline Pt in oxygen-saturated 0.5 M H₂SO₄ at 21 °C; $C_b = 1.3 \times 10^{-6}$ mol/cm³; $D = 1.7 \times 10^{-5}$ cm²/s; $n = 4$; $F = 96487$ C. Note that the potential of the oxygen electrode in a fuel cell is generally between 0.9 and 0.7 V (vs RHE), where $1 \times 10^{-4} < k_f < 1 \times 10^{-2}$ cm/s.

which Q reaches a maximum depends on D_f (Figure 4C). Hence, an indefinite increase of k_f does not help the cause, for reasons beyond the classical assumption that diffusion is the ultimate factor that limits the rate. On the other hand, the maximum charge is realized at smaller values of k_f . Thus, if the objectives are to increase I and Q by increasing the roughness of the electrode surface, then it should be tempered with appropriate changes in k_f .

Experimental Section

Experimental verification of eq 3 was made using the oxidation reaction, $\text{Fe(II)} \rightarrow \text{Fe(III)} + e^-$, on smooth and brush-type gold electrodes. A Kel-F holder held the smooth electrode, exposing 0.283 cm² of the surface to the solution. The brush electrode was similar to the one described by de Levie.²⁷ It was constructed by arranging about 600 parallel strands of 50- μ m-diameter gold wires encased in a heat-shrunk Teflon tubing; only the tip of the 4-mm-long brush was exposed. The area of the brush was estimated by the reduction of adsorbed oxygen²⁴ as 2.45 cm².

The experimental technique involved in the verification of eq 3 was $I-t$ transient (chronoamperometry), which consisted of holding the electrode initially at a potential where there is

no oxidation of Fe(II) and pulsing it to a potential where Fe(II) is oxidized. The initial potential for each transient was 0.53 V vs RHE. A limited number of linear sweep voltammograms (LSV) were measured by using a gold rotating (flat) disk electrode ($G = 0.283$ cm²) and a Pine Instruments AFMRX rotator. $I-t$ transients and Levich-Koutecky plots obtained on the gold disk were used to compute k_f values of the ferrous oxidation. All experiments were conducted at room temperature (21 ± 1 °C) using a Princeton Applied Research (PAR) 273A Potentiostat/Galvanostat and the associated software.

The Fe(II) oxidation on the polycrystalline gold (Au) electrodes was conducted under deaerated conditions in a 125-mL glass cell. The solution, prepared fresh for each experiment, was composed of 5 mM (NH₄)₂Fe(SO₄)₂ in 0.998 M NaClO₄ + 0.002 M HClO₄ (total [ClO₄⁻] = 1 M). It was deaerated by purging with ultrapure N₂ prior to the addition of the ferrous salt and used immediately.

The $I-t$ transient data shown in Figure 1 were obtained by the oxidation of ferrocyanide on stationary Pt electrodes in a nondeaerated aqueous solution of 3 M NaNO₃ containing 15 mM K₄Fe(CN)₆ using a small-volume (2-mL) glass cell. The surfaces of the Pt electrodes were either smooth (polished with alumina powder down to 0.05 μ m), or rough (abraded with 80-

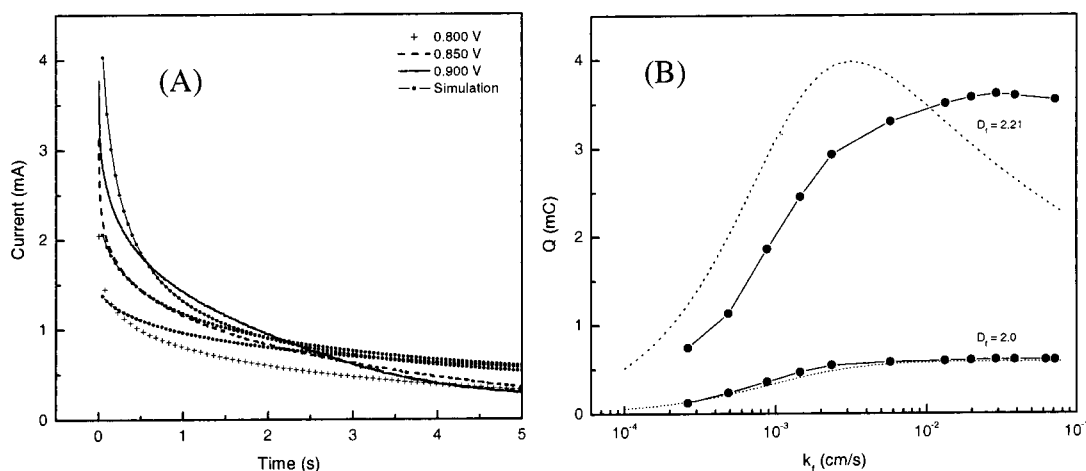


Figure 5. Oxidation of Fe(II) on gold at 21 °C in a deaerated aqueous solution of 5 mM $(\text{NH}_4)_2\text{Fe}(\text{SO}_4)_2$ + 0.998 M NaClO_4 + 0.002 M HClO_4 on a flat electrode (0.283 cm^2) and a brush electrode (2.45 cm^2). (A) I - t transients for the brush electrodes at different potentials as indicated. Note that although the 900 mV transient starts with a higher I than the 850 and 800 mV transients, when $t > 2.5$ s, it has a smaller I . Figure 5 A also shows the simulated transients (—●—) for a porous electrode with $D_f = 2.21$ at k_f 1.259×10^{-3} (bottom), 1.995×10^{-3} (middle), and 5.012×10^{-3} cm/s (top); the transient with the higher k_f has a smaller I at $t > 2.5$ s. (B) Q vs k_f plots for the brush and flat electrodes, experimental (—●—) and simulation (....), obtained by integrating I - t transients between 0.5 and 5 s.

grit SiC powder). The fuel-cell-type porous electrode was assembled by mixing Pt powder (4 mg/cm^2) with Nafion binder (0.5 mg/cm^2) and spreading the mixture on a carbon cloth (Troy). The electrodes were mounted on a Kel-F holder, exposing 0.283 cm^2 of the surface to the electrolyte. A Pt coil served as the counter electrode. A reversible hydrogen electrode (RHE, $\text{Pt}/\text{H}_2(1 \text{ atm})/0.5 \text{ M H}_2\text{SO}_4$) (for experiments in Figure 4), and a $\text{Hg}/\text{Hg}_2\text{SO}_4/\text{saturated K}_2\text{SO}_4$ (for experiments in Figure 1), served as reference electrodes. All potentials were converted to the reversible hydrogen scale.

Results and Discussion

The I - t model described in eq 3 extends the conventional representation of the kinetics on smooth electrodes (eq 1) to rough electrodes.⁶ It is consistent with the time-dependent variation of I proposed by Pajkossy et al.²⁶

Figure 4 represents simulated data using eq 3 and the kinetic parameters that correspond to oxygen reduction on Pt, and it demonstrates the significance of the inclusion of D_f in the flux factor. The simulation assumed an identical initial area ($A = 1 \text{ cm}^2$) for all D_f values. For $D_f = 2$, the I - t transients (Figure 4A) behave similarly to those observed on planar electrodes described by eq 1. For $k_f > 0.5 \times 10^{-2} \text{ cm/s}$, the I - t transients virtually merge with each other. On the other hand, the I - t transients behave differently for $D_f > 2$, with the current increasing with k_f , but only initially. For example, for $D_f = 2.4$ and $k_f > 0.5 \times 10^{-2} \text{ cm/s}$, the increase in I with k_f is observed only when t is close to zero; at longer times, I gets smaller at higher k_f . The limit of k_f when such “reversals” in I take place depends on D_f . The simulation in Figure 4B shows rather dramatic reversals or “crossovers” in current for $D_f = 2.4$; the values I close to time zero are not shown to highlight the effect of k_f on I at t away from zero. The charge, Q , over the entire 100 s (Figure 4C) initially increases with k_f , and becomes a constant for $k_f > 1 \times 10^{-2} \text{ cm/s}$, where the rate is limited by diffusion, but only for $D_f = 2.0$. For $D_f > 2$, Q shows a clear maximum at k_f much smaller than $1 \times 10^{-2} \text{ cm/s}$, much before the rate is limited by diffusion. As k_f increases, the reaction rate is increasingly limited by diffusion. The diffusion layer thickness, δ , increases faster with time at higher D_f , (see the term $[k_f^{(2-D_f)} (D/t)^{(D_f-1)/2}]$ in eq 3), which lowers the I and Q .

For experimental verification of eq 3, we chose the ferrous oxidation reaction because the one-electron transfer is a simple process and because its mechanism and rate parameters have been well investigated.²⁸ We chose gold for the electrode because its surface remains in its elemental state (free of oxide) over the range of potential where ferrous ion is oxidized. Note that the brush electrode does not fall under the strict definition of a “self-similar” fractal surface, but only an approximation to electrodes with $D_f > 2$. To conduct the reaction at various k_f , we subjected the electrode to various electrochemical potentials.² We limited the I - t transient responses to only a few seconds; at longer times ($t > 5$ s), density differences in the volume of the electrolyte close to the electrode may cause convection to compete with, if not dominate, diffusion.

On the smooth gold electrode, in the range of 0.6 to 1.0 V (vs RHE), the I - t transients observed for the reaction $\text{Fe}^{2+} \rightarrow \text{Fe}^{3+} + \text{e}^-$ (data not shown) behaved similarly to the simulated response shown in Figure 4A. The current increased with increasing E (or increasing η) until the rate was under total diffusion control ($E > 1.0 \text{ V}$), above which the transient responses merged with each other. On the brush electrode, I initially reached higher values with an increase in E , but remained so only for a short time (see Figure 5A). At longer times ($t > 2.5$ s), I corresponding to the higher η ($E > 0.85 \text{ V}$) dropped to smaller values than I at the lower η ($E < 0.85 \text{ V}$). Superimposed over the experimental data in Figure 5A are I - t transients simulated using eq 3; kinetic parameters that correspond to Fe(II) oxidation on gold; and $D_f = 2.21$. The match between the simulated data and the experimental data is only reasonably good.²⁹ However, the crossovers in I from higher to lower values with increase in η or k_f can be seen both in the experiments and simulation. The crossovers in I are unique to porous electrodes and are not observed on flat electrodes; they distinguish the I - t transients of electrodes with $D_f > 2$ from those with $D_f = 2.0$.

The crossovers in I observed on the porous electrode are highlighted in Figure 5B by integrating the currents over the periods of 0.5 to 5.0 s of the transients; also included in the figure, for the purpose of reference, are the Q values from the I - t transients for the flat electrode. The k_f values shown in Figure 5 were obtained from the transient and RDE techniques described under the Experimental Section. Note that for the

brush electrode, Q increases initially with k_f , but reaches a maximum around 2×10^{-2} cm/s (900 mV) and begins to decrease at higher k_f . On the other hand, Q for the flat electrode reaches maximum at about 1×10^{-2} cm/s and stays constant at higher k_f . The reason for the maximum seen on the brush electrode is due to the crossovers of the current to lower values at higher k_f , especially at longer t . We have also seen similar crossovers in current and maximum in Q for oxygen reduction on a Pt brush electrode.³⁰

The experimental data in Figure 5A,B are limited, at least to some degree, by two factors. At $t < 0.5$ s, the charging of the double layer capacitance is a major source of interference to the current, I , especially for a brush electrode whose area is large. At $t > 5$ s, diffusion may not be the only source of mass transport of the reactant to the electrode surface. Therefore, generating experimental evidence to verify eq 3 is limited to transients over short periods of only a few seconds. Even within these limits, the I - t transients on the flat and brush electrodes behaved as predicted by eq 3. The mismatch between the experimental and simulated data is largely due to the above-mentioned limitation and that the brush electrode is not a truly fractal electrode, but only an approximation to an electrode with $D_f > 2$. However, there is a reasonably good match between the experimental and the simulated data, including the crossovers in I and the maximum in Q .

Conclusion

Equation 3 is a generalized model for the rate of electrochemical reactions on flat and porous electrodes. The adaptation of the dimension-dependent flux⁸ extends the classical electrochemical expression eq 1, originally derived for planar electrodes, to porous electrodes. It reveals a fundamental dependency of current, I , and charge, Q , on dimension D_f , and rate constant k_f . The equation applies over the entire range of scenarios: activation/no diffusion, partial activation/partial diffusion, and diffusion/no activation. The model emphasizes that dimension D_f , more than true area A , determines the behavior of I versus k_f .

The oxygen reduction simulation in Figure 4 provides a specific example in which eq 3 predicts the kinetics of a partial-diffusion-limited reaction on porous electrodes. In a fuel cell, the cathode is generally porous and has a dimension, $D_f > 2$, for which the rate of increase of the diffusion layer thickness with time depends on D_f , and rate constant, k_f , which does not allow the current to be higher at higher k_f at all times. Typically, with increase in k_f , the I at long times reverses to lower values than the I at smaller k_f ; such a reversal is absent if the electrode surface is flat ($D_f = 2$). On a porous electrode, the lowering of I causes the charge, Q , to increase initially with k_f and decrease at higher k_f , showing a peak in the Q vs k_f behavior. The peak in Q occurs much before the k_f is so large that the reaction rate is limited by diffusion. No such peak is observed on a flat electrode, where Q reaches a maximum, typically for $k_f > 1 \times 10^{-2}$ cm/s and the rate is limited by diffusion; Q remains constant with further increase in k_f .

The ferrous oxidation reaction described in this work provides a simple example to demonstrate the interactions among geometric dimension, activation energy, and diffusion. The brush electrode used for the demonstration is not a fractal electrode in the strict sense of self-similarity. The brush electrode is an approximation to an electrode with $D_f > 2$, and the I - t transients obtained using it demonstrate that the current crossovers from higher to lower values at higher overpotential (or higher rate

constant) on the porous electrode, not seen on the flat electrode. In earlier studies, we have shown that the organic adsorbates 2,4-dimethoxy pyrimidine and 1,3-dimethyl uracil, in an apparent contradiction, slow the rate of electrochemical reduction of oxygen on a flat Pt electrode,³¹ but increase the current on a porous catalyst-type Pt electrode.¹⁹ A model similar to the one described by eq 3 resolves this paradox.

Acknowledgment. Dr. Terry Phillips of The Johns Hopkins University Applied Physics Laboratory (JHU/APL) and Professor Robert de Levie of Bowdoin College, Maine, provided valuable comments. We acknowledge Mr. Benjamin Walker for editorial help, and the JHU/APL Independent Research and Development program for financial support.

References and Notes

- (1) Sapoval, B. In *Fractals and Disordered Systems*; Bunde, A., Havlin, S., Eds.; Springer-Verlag: New York, 1991; Chapter 6, p 207.
- (2) The forward rate constant, k_f , can be expressed in terms of a standard rate constant (k_0) and overpotential (η) as $k_f = k_0 \exp(-\alpha nF/RT\eta)$, where α , n , F , and R are constants and T is the temperature. $\eta = (E - E_{eq})$, where E_{eq} is the equilibrium potential and E is the applied potential.
- (3) Bard, A.; Faulkner, L. *Electrochemical Methods*; John Wiley & Sons: New York, 2001; p 231.
- (4) Macdonald, D. D. *Transient Techniques in Electrochemistry*; Plenum Press: New York, 1977; p 20.
- (5) Tarasevich, M. R.; Sadkowsky, A.; Yeager, E. In *Comprehensive Treatise of Electrochemistry*; Conway, B. E., Bockris, J. O'M., Yeager, E., Khan, S. U. M., White, R. E., Eds.; Plenum Press: New York, 1983; Vol. 7, Chapter. 6.
- (6) de Levie, R.; Vogt, A. *J. Electroanal. Chem.* **1990**, 281, 23.
- (7) Nyikos, L.; Pajkossy, T. *Electrochim. Acta* **1986**, 31, 1347.
- (8) de Levie, R. *J. Electroanal. Chem.* **1990**, 281, 1.
- (9) Kant, R.; Rangarajan, S. *J. Electroanal. Chem.* **1994**, 368, 1.
- (10) Sapoval, B.; Filoche, M.; Karamanos, K.; Brizzi, R. *Eur. Phys. J. B* **1999**, 9, 739.
- (11) Pajkossy, T.; Nyikos, L. *Phys. Rev. B* **1990**, 42, 709.
- (12) Pajkossy, T.; Nyikos, L. *J. Electrochem. Soc.* **1986**, 133, 2061.
- (13) Filoche, M.; Sapoval, B. *Eur. Phys. J. B* **1999**, 9, 755.
- (14) Kant, R.; Rangarajan, S. *J. Electroanal. Chem.* **1995**, 396, 285.
- (15) Oldham, K. B. *J. Electroanal. Chem.* **1991**, 297, 317.
- (16) de Levie, R. In *Advances in Electrochemistry and Electrochemical Engineering*; Delahay, P., Tobias, C. W., Eds.; John Wiley & Sons: New York, 1967; Vol. 6, p 329.
- (17) Pajkossy, T. *J. Electroanal. Chem.* **1991**, 300, 1.
- (18) Pajkossy, T. *Heterogeneous Chem. Rev.* **1995**, 2, 143.
- (19) Saffarian, H.; Srinivasan, R.; Chu, D.; Gilman, S. *J. Electrochem. Soc.* **2001**, 148, A559.
- (20) Bard, A.; Faulkner, L. *Electrochemical Methods*; John Wiley & Sons: New York, 2001; p 195.
- (21) Macdonald, D. D. *Transient Techniques in Electrochemistry*; Plenum Press: New York, 1977; p 78.
- (22) Bard, A.; Faulkner, L. *Electrochemical Methods*; John Wiley & Sons: New York, 2001; p 163.
- (23) Macdonald, D. D. *Transient Techniques in Electrochemistry*; Plenum Press: New York, 1977; p 72.
- (24) Trasatti, S.; Petrii, O. A. *Pure Appl. Chem.* **1991**, 63, 711.
- (25) Bard, A.; Faulkner, L. *Electrochemical Methods*; John Wiley & Sons: New York, 2001; p 191–196.
- (26) Imre, A.; Pajkossy, T.; Nyikos, L. *Acta Metall. Mater.* **1992**, 40, 1819.
- (27) de Levie, R. *Electrochim. Acta* **1964**, 9, 1231.
- (28) Anson, F. *Anal. Chem.* **1961**, 33, 934, 939.
- (29) The brush electrode described in this work and brush and powder electrodes described in the literature,^{6,24,27} are only approximations to electrodes with fractal geometry. There is no known way of making an electrode with $2 < D_f < 3$ that also conforms to the strict definition of the self-similarity of fractal geometry. Hence the match between the experimental and simulated data is not perfect. Furthermore, at long times ($t > 5$ s), the experimental data do not represent an ideal diffusion process since nondiffusional processes including convection may begin to contribute to the mass transfer process.
- (30) Srinivasan, R.; Saffarian, H. Unpublished work.
- (31) Saffarian, H.; Srinivasan, R.; Chu, D.; Gilman, S. *J. Electroanal. Chem.* **2001**, 504, 217.